Available on CMS information server

CMS CR -2009/337

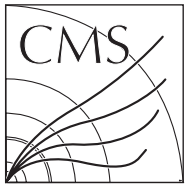

The Compact Muon Solenoid Experiment

Conference Report

Mailing address: CMS CERN, CH-1211 GENEVA 23, Switzerland

11 November 2009 (v2, 18 November 2009)

The CMS Strip Tracker Calibration, Methods and Experience with Cosmic Ray Data

Gordon Kaussen for the CMS Collaboration

Abstract

The CMS Silicon Strip Tracker (SST) needs to be precisely calibrated in order to correctly interpret and reconstruct the events recorded from the detector, ensuring that the SST performance fully meets the physics research program of the CMS experiment. Calibration constants may be derived within several workflows, from promptly reconstructed events with particles as well as from commissioning events gathered just before the acquisition of physics runs. These calibration procedures have been exercised in summer 2008 and 2009, when the CMS detector has been commissioned using cosmic muons with and without magnetic field. In this paper the reconstruction strategies, the calibration procedures and the detector performance results from the latest CMS operation are described.

Presented at *IEEE2009: 2009 IEEE Nuclear Science Symposium and Medical Imaging Conference*

The CMS Strip Tracker Calibration, Methods and Experience with Cosmic Ray Data

Gordon Kaußen, on behalf of the CMS Collaboration

***Abstract*—The CMS Silicon Strip Tracker (SST) needs to be precisely calibrated in order to correctly interpret and reconstruct the events recorded from the detector, ensuring that the SST performance fully meets the physics research program of the CMS experiment. Calibration constants may be derived within several workflows, from promptly reconstructed events with particles as well as from commissioning events gathered just before the acquisition of physics runs. These calibration procedures have been exercised in summer 2008 and 2009, when the CMS detector has been commissioned using cosmic muons with and without magnetic field. In this paper the reconstruction strategies, the calibration procedures and the detector performance results from the latest CMS operation are described.**

I. Introduction

THE Compact Muon Solenoid (CMS) experiment [1] is one of the four main detectors placed at the Large Hadron Collider (LHC) based at CERN, Switzerland. It is a general purpose collider detector consisting of a superconducting solenoid which provides a $3.8\,\mathrm{T}$ magnetic field and hosts the tracking detectors and the electromagnetic and hadronic calorimeters. Beyond the magnet an iron return yoke and a muon tracking system are placed.

The tracking detector consists of a three layer silicon pixel device placed close to the interaction region and a silicon strip tracker (SST) [2] surrounding the pixel detector and covering the pseudorapidity region $|\eta| < 2.5$. The SST is $5.5\,\mathrm{m}$ long with a $2.2\,\mathrm{m}$ diameter and is composed of 15,148 microstrip detectors, called modules. With its 9.6 million readout channels and a total of $198\,\mathrm{m}^2$ of silicon active area it is the largest silicon tracker ever built.

The tracker is organized in four subdetectors, two barrels (inner barrel TIB and outer barrel TOB) and two endcaps (inner disk TID and endcap TEC). The TIB and the TOB are cylindrical structures coaxial with the beam axis and consist of four and six layers, respectively, at different radii. The TID and the TEC form the endcap of the inner barrel and the whole tracker, respectively, and are divided in disks (three for the TID and nine for the TEC) orthogonal to the beam axis. Modules placed on the endcaps are organized in up to seven rings with different radii. In total 15 module geometries are used in the strip tracker differing mainly in the active thickness ($320\,\mu\mathrm{m}$ and $500\,\mu\mathrm{m}$, respectively), in the microstrip pitch (ranging from $80\,\mu\mathrm{m}$ to $183\,\mu\mathrm{m}$) and in shape (rectangular in the barrel region and trapezoidal in the endcaps). In addition to the so-called mono or $r\phi$ modules allowing a 1-dimensional position measurement perpendicular to the strips, some layers and rings are equipped with so-called stereo modules delivering a 2-dimensional hit measurement.

The readout of each module is performed by the chip APV-25 [3]. The chip takes as input 128 analog channels, each one connected to a strip, and sends the sampled signals, stored temporarily in a pipeline, to the Analog Opto-Hybrid device (AOH). Each AOH converts the multiplexed electronic signals coming from two APV-25 in optical signals, and transmits them to the off-detector front-end readout system (Front End Driver) via optical fibres. On each module 4 or 6 APV-25 are mounted, depending on the number of detector strips, connected with 2 or 3 AOH, respectively.

At a bunch crossing rate of $40\,\mathrm{MHz}$ and a design luminosity of $10^{34}\,\mathrm{cm}^{-2}\mathrm{s}^{-1}$ about 10^9 interactions will occur every second. To reduce this huge amount of data, a level 1 trigger based on custom-made electronics and a software based high level trigger will select only events with specific signatures. The final event rate will be of the order of $100\,\mathrm{Hz}$.

II. Data Samples

The analysis presented in this paper are based on the global cosmic run data collected in 2008 and 2009, respectively. In these so-called CRAFT (Cosmic Runs At Four Tesla) all subdetectors of CMS were read out simultaneously for several month using the muon system as trigger for cosmic muons with a rate of about $400\,\mathrm{Hz}$. In addition, calorimeter and random triggers were used to exercise high rate runs in the order of $10\,\mathrm{kHz}$.

In total, about $270\,\mathrm{M}$ ($480\,\mathrm{M}$) muon events were collected in CRAFT08 (CRAFT09), out of which about $6\,\mathrm{M}$ ($12\,\mathrm{M}$) events contained a reconstructed track in the strip tracker.

In $\sim 90\,\%$ ($\sim 93\,\%$) of the global data taking time in 2008 (2009) the strip tracker participated in the operation. During this time, both runs with nominal magnetic field ($3.8\,\mathrm{T}$, $\mathrm{B_{on}}$) and zero magnetic field ($0\,\mathrm{T}$, $\mathrm{B_{off}}$) were performed. During CRAFT08, only the so-called peak readout mode of the APV front end chip was used. This mode provides a high signal-to-noise (S/N) ratio with the pulse having a risetime of $50\,\mathrm{ns}$ and a signal above threshold for about 7 bunch crossings (the time between two consecutive bunch crossings is $25\,\mathrm{ns}$). During CRAFT09, instead, the first half of data taking was operated in peak mode, while the second half was performed in the so-called deconvolution mode. The latter will be the nominal read out mode for collisions and was used for the first time. With a pulse risetime of $25\,\mathrm{ns}$ and a fast signal shaping it

Manuscript received November 19, 2009. This work was supported in part by the German Federal Ministry of Education and Research BMBF, and by the Helmholtz Alliance "Physics at the Terascale".

G. Kaußen is with the University of Hamburg, Hamburg, Germany (e-mail: gordon.kaussen@cern.ch).

is optimized to reduce the pile-up of events during collision operation. Instead, since the cosmic muons arrive randomly with respect to the LHC clock, this readout mode results in off-time particles with reduced signal response when used in cosmic data taking. Therefore, only the peak mode data of CRAFT09, that are less sensitive to off-time particles due to the long pulse shape, are used in this paper.

In addition, for the channel status calibration the random trigger events are used to analyse the noise occupancy without any particle contamination. Since the probability to trigger a cosmic muon randomly is very low, a uniform occupancy accross all tracker layers can be assumed using these noise events.

It has to be taken into account that cosmic data are differing from collision data in several aspects. First of all, the illumination of the detector and thus the statistic is not uniform resulting in varying calibration precision accross the tracker. Moreover, the random arrival time of the cosmic muons leads to a trigger jitter affecting the effective signal height. Large angles of incidence with respect to the single module surface have an impact on quantities like cluster charge, cluster size and position resolution, too. Finally, there is no beam spot constraint, which requires a specially adapted event reconstruction and makes for example the seeding during track reconstruction more sensitive to noisy components. All analysis based on cosmic muon data therefore need a careful cluster, hit and track selection as described in the following sections.

III. Low Level Reconstruction

The data reconstruction and analysis are performed within the CMS software framework called CMSSW. It is structured in a modular architecture and thus provides a large number of plug-in modules that can be adapted to raw data or higher-level reconstructed data as input. The basis of the framework is the Event Data Model (EDM) where all the user-defined types are contained within a single object referred to as the event. It contains the information of all detectors read out at a certain trigger.

In addition to the event data themselves, so-called non-event data are essential for the reconstruction. These condition data (e.g. pedestal and noise of each strip in the SST, information about cabling, gain, Lorentz angle, channel status etc.) are provided by an independent object called the event setup. It is populated during event processing by accessing an Oracle database called ORCOF in which all condition data needed for the offline event reconstruction are stored. The modules to be executed in the reconstruction chain and their schedule are defined in a CMSSW path. They interact directly with the event and the event setup.

The low level reconstruction chain is schematically represented in figure 1. The first module during reconstruction unpacks the raw data received from the front-end electronics using the cabling information from the condition database and reorders them by grouping strips belonging to the same silicon detector together. These are the so-called *Raw Digis*.

They are further processed by subtracting the pedestal, correcting for the common mode (which is a uniform shift of the signal level of adjacent strips event by event due to noise) and suppressing zero signal strips. Usually these steps are already performed in the front-end eletronics. The offline procedure is mainly used for commissioning purposes. The zero-suppressed data are called *Digis*.

The next step contains the clusterizer which groups adjacent strips above certain signal-to-noise thresholds (after gain calibration) to form a *Cluster*. The position measurement is derived by calculating the centroid of the resulting cluster. Masked strips are removed in the clusterizer and their data are not taken into account.

Finally, each cluster is associated with a reconstructed hit, called *RecHit*, owing its position to the cluster centroid. In case of a magnetic field the RecHit position is additionally corrected for the Lorentz shift. The hit coordinates can then be converted from local module coordinates in CMS global coordinates and used for the following tracking procedure.

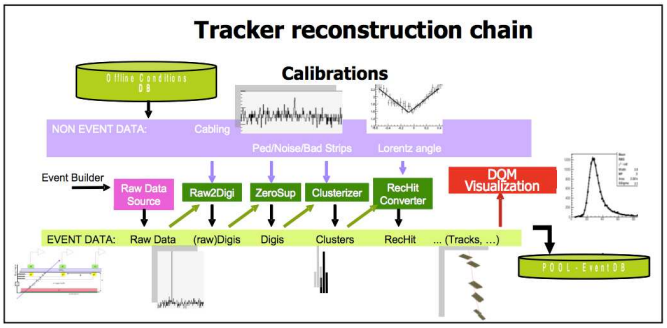

Fig. 1. Block diagram of the low level reconstruction in the SST.

IV. Calibration Workflow

To provide up-to-date conditions already for the prompt reconstruction of the full physics dataset at the Tier-0 (which is the computing facility at CERN performing the express and prompt reconstruction), several data streams are maintained from the CMS experiment site at the so-called Point 5 (see figure 2). Besides the physics stream, which contains the full

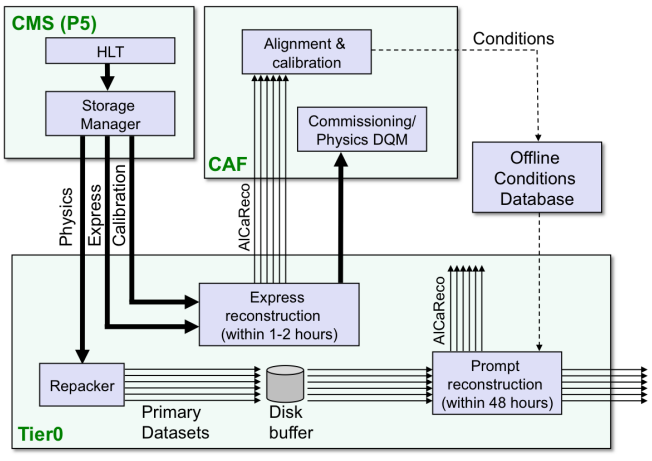

Fig. 2. Schematic view of the express reconstruction, prompt reconstruction and calibration workflow in CMS.

statistics of events selected by the High Level Trigger (HLT), both an express and a calibration stream are transferred to the Tier-0 [4].

The express stream is a skim of the physics stream with reduced statistics (about $10\,\%$ of the total data bandwidth). It is intended to be used for fast alignment and calibration analysis and to provide fast feedback for physics analysis.

The calibration stream is also a reduced stream of about $10\,\%$ of the total bandwidth and contains mostly hardware calibration data for example for pedestal and noise calibration. This stream will not be discussed in this paper.

The express stream is reconstructed at the Tier-0 within a delay of 1-2 hours with respect to data taking. Based on this express reconstruction, dedicated skims called *AlCaReco* are produced. Each AlCaReco dataset is used for a special alignment or calibration procedure and thus contains only dedicated events selected according to the HLT trigger bit and a reduced event content that is needed for the calibration.

The AlCaReco skims are transferred to the CERN Analysis Facility (CAF) where they are used as input for the alignment and calibration algorithms operated with short latency. Within 24 hours a new set of updated conditions should be completed and validated. Afterwards, these constants are uploaded to the condition database.

During the prompt calibration loop, the primary datasets consisting of the raw data arriving from the experiment are stored on a disk buffer at the Tier-0. After a delay of up to 48 hours the first reconstruction of the full physics dataset, called *prompt reconstruction*, is performed using the updated conditions. Finally, these reconstructed data can be passed to the physics analysis.

V. Calibration Results

A. Gain Calibration

When traversing a depleted silicon sensor, a charged particle releases charge carriers in the sensor. Collecting these charge carriers, the energy deposited by the primary particle inside the detector can be measured. Since this measurement comprises several components, namely the silicon sensor itself, the APV front end chip, the Analog Opto-Hybrid and the Front End Driver, the response obtained with different modules can vary, depending on the performance of the mentioned components. Therefore, it is important to know and to calibrate the gain, which corresponds to the ratio of the measured ADC counts after digitization in the FED and the charge produced in the silicon sensor, for each readout chain.

The eletronic part of the readout chain can be calibrated using the height of the APV digital signal called tick mark. The tick mark is a synchronisation signal that is sent every 70 bunch crossings by the APV and its digitized height is a measure for the electronics gain. In dedicated commissioning runs called timing runs this signal is determined for each APV. The corresponding gain factor, which is the tick mark height normalized to a reference height of 640 ADC counts, is stored in the condition database and can be applied during cluster reconstruction to unify the measured signal and noise with respect to the electronics gain.

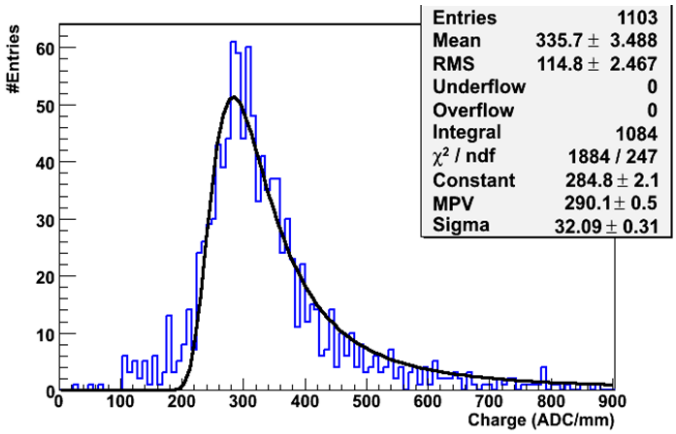

Fig. 3. Cluster charge distribution for a strip tracker module. Each cluster charge is normalized to the path length of the corresponding particle in the silicon. The result of a Landau fit is shown (solid line).

However, the ultimate calibration, necessary for particle identification techniques using energy loss in the silicon detectors, can only be obtained by using the signals produced by particles. It takes into account for example non-uniformities in the silicon, which is not considered in the tick mark procedure.

The particle gain calibration uses the charge information of clusters associated to a reconstructed muon track. Normalizing this cluster charge to the path length of the particle in the silicon sensor, a charge distribution can be obtained for each module by collecting all clusters reconstructed in the respective detector. Since the charge released in thin material layers is known to be Landau distributed, such function can be fitted to the data. In figure 3 the cluster charge distribution with the fitted Landau curve is shown for a single module.

The gain factor is determined by normalizing the most probable value (MPV) of the Landau distribution to 300 ADC counts/mm, which is the value expected for a minimum ionizing particle [5]. These inter-calibration constants are stored in the condition database and can be applied to each cluster reconstructed in the respective module.

During CRAFT operation, only tracks with a momentum of $p > 1\,\mathrm{GeV/c}$ were used for this calibration. In addition, each module had to have at least 50 hits to be taken into account since less statistics results in an useless Landau fit. Using about $1\,\mathrm{M}$ cosmic tracks, the gain factor could be measured for $90\,\%$ of the strip modules. The remaining modules where the statistic was too low or the fit failed received a calibration constant of 1. Since the available statistic in collision operation will be much higher, the gain calibration will be performed on a single APV level instead of the module level described here.

In figure 4 the distribution of the MPVs obtained with the Landau fits is shown, subdivided by sensor thickness. Figure a) displays the distribution for uncalibrated data with a spread of about $10\,\%$. Applying the electronics gain calibration based on the tick mark information, the resulting response of the modules is already more uniform, as can be seen in figure b). Finally, applying the gain factor derived from particles using uncalibrated data (since this procedure corrects also for the electronics gain automatically), the distribution shown in figure

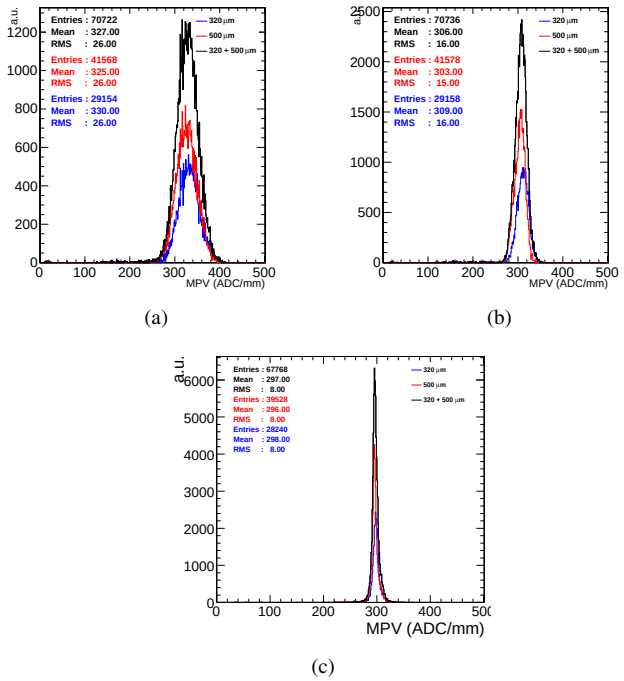

Fig. 4. Distritubions of the MPVs, obtained with Landau fits to the normalized cluster charge distribution of each single module, for thin sensors (blue), thick sensors (red) and the sum (black). a) Uncalibrated data (CRAFT09), b) tick mark calibration applied (CRAFT09), c) particle calibration applied (CRAFT08).

c) is obtained. The residual spread of about 3 % is dominated by the error on the MPV fit. The result displayed in figure c) can also be achieved by applying on top of the tick mark calibration the remaining gain derived from particles. In this case, the gain from particles has to be used together with the gain from tick marks since it corrects only for the remaining non-uniformities.

B. Lorentz Angle Calibration

Since the strip tracker is operated in a 3.8 T magnetic field parallel to the beam axis, the electric (**E**) and magnetic (**B**) field vectors are perpendicular to each other inside the barrel modules (see figure 5). This causes the charge carriers produced in the n-bulk silicon of both the inner and the outer barrel detectors to undergo a Lorentz force in addition to their drift to the readout strips (p^+) along the electric field. The resulting deflection is perpendicular to the drift direction and leads to a shift of the measured cluster position with respect to the real impact point in the sensitive coordinate x. This shift can be parameterized by the so-called Lorentz angle θ_L, which is the angle between the electric field direction and the overall drift direction of the charge carriers.

In order to reconstruct the real hit position, the Lorentz angle, which depends on the electric and magnetic fields, the temperature and the absorbed radiation dose, has to be precisely measured and the reconstructed cluster position has to be corrected for this effect accordingly. It can be measured by determining the track incident angle with respect to the module surface for which the minimum cluster width is achieved [6]. In case of no magnetic field, this minimum is

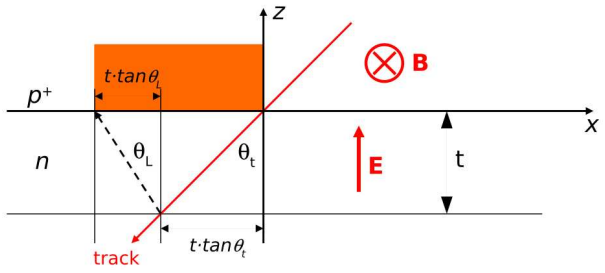

Fig. 5. Cross section of a barrel module with thickness t. The sensitive coordinate (perpendicular to the strips) is along x, while z is perpendicular to the module surface. Due to the Lorentz angle θ_L the measured cluster width (orange area) is widened in this example.

observed for perpendicular incidence (the Lorentz force and the Lorentz angle are zero). In case of $B > 0\,\mathrm{T}$, the minimum is obtained when the incident angle is equal to the Lorentz angle because the charge carriers drift parallel to the track direction.

Figure 6 shows an example of the measured cluster width as a function of the tangent of the track indicent angle for a TOB layer 4 module. To extract the Lorentz angle, the following function is fitted to the data [5]:

$$f(\theta_t) = \frac{t}{p} \cdot p_1 \cdot |\tan\theta_t - p_0| + p_2$$

where t is the thickness of the sensor, p is the pitch of the strips and p_0, p_1 and p_2 are the fit parameters. p_0 represents the tangent of the Lorentz angle, p_1 is the product of the slope of the line and the ratio of thickness and pitch and p_2 is the average cluster size at the minimum.

This measurement was performed for each barrel module with enough statistics (at least 1000 hits associated to a track). Afterwards, the distribution of all measured values in a given layer is produced and the mean and sigma of a Gaussian fit are extracted. This mean Lorentz angle is then assigned to each

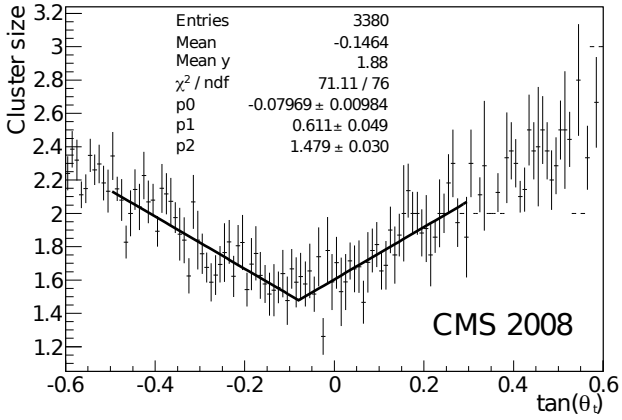

Fig. 6. Measured cluster size (in number of readout strips) as a function of the tangent of the track incident angle for a TOB layer 4 module with 3.8 T magnetic field. The minimum of the fit function (solid line) represents the Lorentz angle.

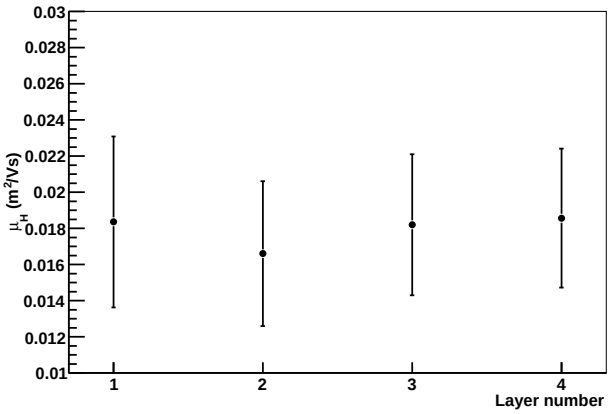

(a)

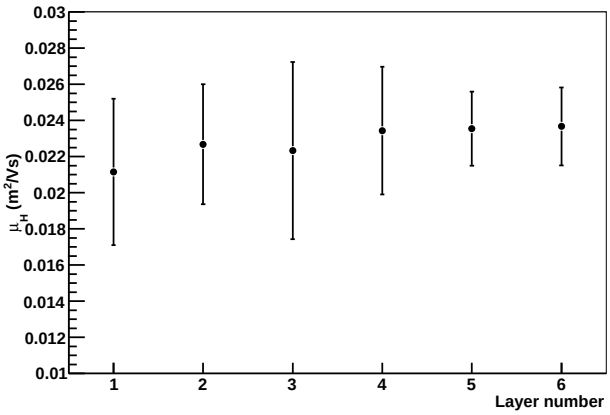

(b)

Fig. 7. Mean value of the Hall mobility μ_H derived from a Gaussian fit for all TIB layers a) and all TOB layers b), respectively. The error bars correspond to the RMS of the respective gaussian distribution.

module in the respective layer since the cosmic track statistic was too low to calibrate each module separately with high precision.

Figure 7 shows the mean values for the Hall mobility μ_H, which is the tangent of the Lorentz angle normalized to the magnetic field $\mu_H = \tan\theta_L/B$, for all TIB layers (a)) and all TOB layers (b)), respectively, as measured during CRAFT08. The errors represent the RMS of the respective layer distributions. The measurements are consistent within the different layers of the inner and the outer barrel and differ between TIB and TOB mainly due to the different sensor thickness.

These results were also used in the alignment studies for the strip tracker since the shift of the cluster position due to the Lorentz angle clearly affects the alignment of the modules which is more precise than this shift and thus has to be taken into account [7].

C. Channel Status Calibration

For the event reconstruction the knowledge of both dead and noisy components in the tracker is crucial to avoid inefficiencies during track reconstruction and the creation of fake tracks. This information is accessed from different sources. During commissioning a list of active detectors included in the readout is provided and dead components are subsequently masked in the condition database. In addition, the Detector Control System (DCS) delivers the high and low voltage status of each strip module. Detectors for which an error was observed by the front-end driver (e.g. the loss of the synchronization with respect to the LHC clock) are moreover automatically removed event by event by the raw data unpacker. Finally, noisy or *hot* components can be spotted in a specially adapted offline calibration workflow.

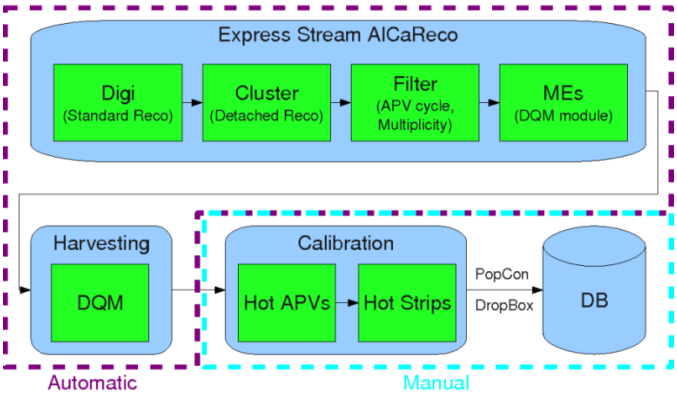

Fig. 8. Schematic view of the channel status calibration workflow for the strip tracker.

The channel status calibration is based on the analysis of the cluster occupancy of single strips and entire readout chips to identify hot components. A dedicated AlCaReco skim is used as input containing the cluster collection of the whole strip tracker and differing from the standard reconstruction by removing only known bad components from commissioning analysis but not from former channel calibration. Since the channel status may change from run to run (e.g. due to a repaired high voltage power supply), this offline analysis has to be performed for each run from scratch to allow the recovery of bad components. Therefore, it is operated in the prompt calibration loop providing an updated channel status for the

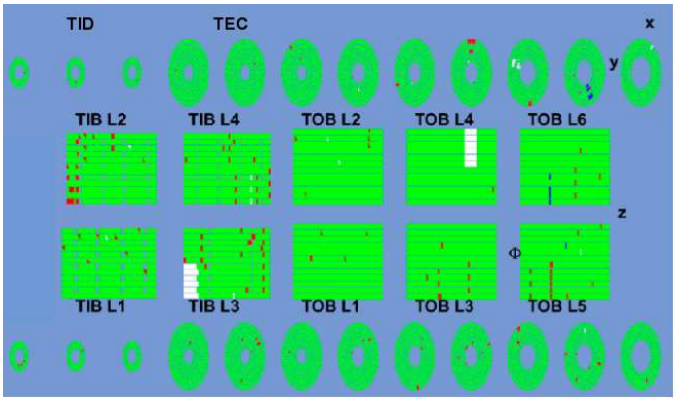

Fig. 9. Tracker map for the strip tracker indicating the channel status during CRAFT09 as obtained by the commissioning analysis: Working modules (green), disabled (white), not read-out (blue), other (mainly missing HV) (red).

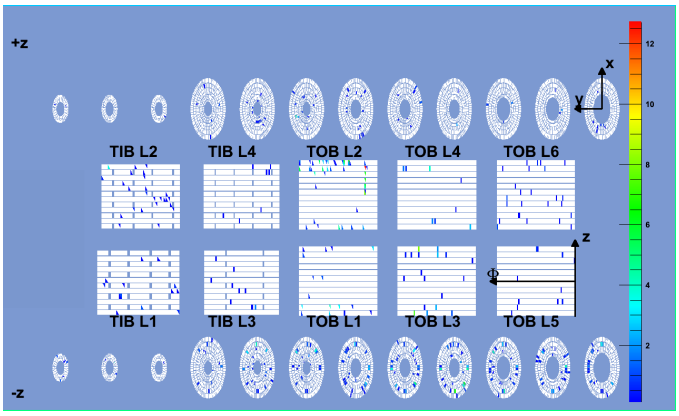

Fig. 10. Tracker map for the strip tracker indicating the percentage of hot strips per module for a particular run in CRAFT09 as identified with the channel status calibration using an absolute occupancy threshold of 10^{-4}. White means that no hot strip was found.

prompt reconstruction of the respective run.

For each silicon module an occupancy histogram is produced after filtering some events that are known to be noisy in special bins of the APV readout cycle and that could bias the hot component identification. This procedure is fully automatic and schematically viewed in figure 8.

The analysis of the cluster occupancy itself is operated in a by-hand procedure which is foreseen to be automated in the future. It consists of two main steps: First the identification of hot APVs and second the identification of single hot strips.

The APV occupancy is analyzed by comparing the median occupancy of all strips belonging to the same readout chip with the mean of the median occupancies of all APVs in the same layer (disk) and the same z region (ring) for the barrel (endcap). Thus, a uniform occupancy in the same η region is assumed. The median is used instead of the mean to reflect the behaviour of the entire APV avoiding a bias by single hot strips. If both this relative occupancy and in additon the absolute occupancy (measured with respect to the total number of events) exceed certain thresholds, the respective APV is masked as bad.

Afterwards, the single strip occupancy is analyzed skipping the already masked APVs. Assuming a poissonian probability for a given strip occupancy based on the mean occupancy of the corresponding readout chip, the hot channel identification is performed in an iterative procedure removing bad strips from the next loop. In addition to this relative occupancy, again an absolute occupancy threshold is taken into account to mask a strip as hot.

All masked components, both readout chips and single strips, are uploaded to the condition database and removed in the prompt reconstruction accordingly.

In figure 9 a so-called tracker map is shown for the strip tracker summarizing the channel status during CRAFT09 as delivered by the various sources of information mentioned above. Each silicon module is represented by a rectangle (trapezoid) in the barrel (endcap) region and one component of a double-sided module constitutes one half of this area. All working modules are shown in green while the disabled ones are white. The latter are dominated by a closed cooling loop in layer 3 of the TIB and a control ring in layer 4 of the TOB not working. The corresponding modules are removed from the cabling. Detectors that are not read out are indicated in blue and are mainly affected by broken optical fibers, which means that only a fraction of the respective module is not working. The red modules are suffering other problems mostly related to missing high voltage. All in all, the operational fraction of the strip tracker was $98.1\,\%$.

In addition, figure 10 displays the tracker map as obtained by the channel status calibration for one particular run. The color palette indicates the percentage of a module that was masked as hot in the analysis where white means that no hot strip was found in the respective detector. Using an absolute occupancy threshold of 10^{-4} for the cosmic runs, the fraction of components masked offline is in the order of $0.1\,\%$.

D. Hit Efficiency Calibration

In addition to the bad components identified during commissioning and offline calibration, the measurement of the hit reconstruction efficiency is a useful method to discover missing modules not identified in the previous phases of the bad component search. This analysis has been performed using the cosmic data of CRAFT08 and CRAFT09.

Only high quality tracks are selected for this study, which means that the event contains only a single track with at least eight hits and a maximum of four lost hits. In addition, the track trajectory is required to pass through the center of a module (i.e. at least five sigma from the sensor edge) to avoid inefficiencies due to the limited size of the sensor. If these requirements are fulfilled, it is searched for a hit that is compatible with the reconstructed track on each module crossed by the trajectory. The single module hit efficiency is derived by counting the number of events where a corresponding hit was found with respect to the total number of events analyzed for the respective module.

In figure 11 the inefficiency (which is the number of missing hits compared to the total number of expected hits) is shown

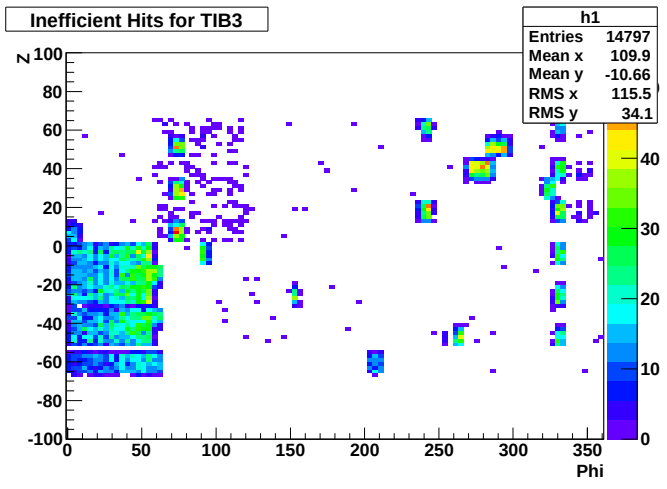

Fig. 11. Location of missing (inefficient) hits in TIB layer 3. The structure reflects the pattern of known bad modules from commissioning.

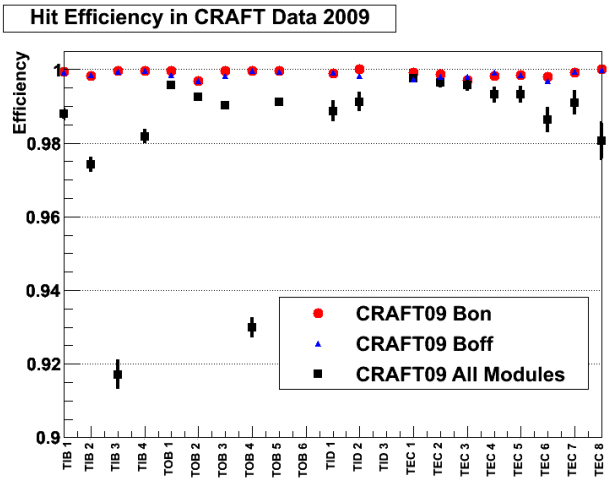

Fig. 12. Average module hit reconstruction efficiency for the various layers and disks in the strip tracker as measured with CRAFT09 cosmic data. The black squares include all modules, while the red circles (B on) and blue triangles (B off) show the results after masking of known faulty modules.

as an example for all modules located in the TIB layer 3. The inefficient regions spotted by this analysis match exactly the known bad modules from commissioning analysis displayed in figure 9 for the respective layer. Thus, the hit efficiency study can re-find known bad components and be used by implication to identify new regions of problematic modules.

Carrying out the procedure for all different layers in the barrel region and all disks in the endcaps, respectively, and averaging the corresponding module hit efficiencies, the distribution shown in figure 12 is obtained for CRAFT09 data. The black points indicate the results before removing known faulty components from the analysis. The average hit finding efficiency is about $98.2\,\%$ with some outliers down to $\sim\ 92\,\%$. After masking the faulty modules (red circles for B field on data, blue triangles for B field off data), the efficiency increases to an average of about $99.9\,\%$ among all the layers. It is obvious that no significant changes in efficiency are observed with the magnetic field on or off.

The hit efficiency study will be adapted to be used in the calibration workflow to provide an additional method for identifying and masking of faulty modules for the subsequent event reconstruction.

VI. Conclusions

The global cosmic runs in 2008 and 2009, denoted as CRAFT08 and CRAFT09, respectively, provided a unique opportunity to commission the entire CMS experiment and to gain experience in operating all detector parts already before the collision runs have started.

Using the muon system as trigger for cosmic muons, more than $700\,\mathrm{M}$ cosmic events could be collected providing particle tracks to all subdetectors including millions of muons passing the strip tracker.

These particles could be efficiently reconstructed using event reconstruction algorithms specially adapted to the needs of cosmic particles not originating from the interaction point. The reconstructed data were used to exercise and to perform several workflows delivering updated calibration constants either in time for the prompt reconstruction and thus fulfilling the prompt calibration loop or for several reprocessings of the datasets to improve the detector understanding and the quality of the event reconstruction.

For the strip tracker these calibration workflows consisted of the gain calibration resulting in measured gain factors for about $90\,\%$ of the modules, the Lorentz angle calibration providing a Lorentz angle value for each single barrel layer, the channel status calibration delivering an updated list of hot components for each single run and the hit efficiency analysis with an overall hit reconstruction efficiency of about $99.9\,\%$.

These results show that the cosmic runs were very successful exercises for the CMS experiment underlying the excellent performance of the detector and providing very important experience for the commissioning and the preparation for collision operation.

References

[1] CMS Collaboration. *The CMS experiment at the CERN LHC*, JINST 3 (2008) S08004.

[2] CMS Collaboration. *The Tracker Project Technical Design Report*, CERN/LHCC 98-6, April 15, 1998.

[3] Lawrence Jones. *APV25-S1 User Guide.* RAL Microelectronics Design Group, Version 2.2, 2001.

[4] D. Futyan. *Commissioning the CMS Alignment and Calibration Framework*, Proceedings for the 17th International Conference on Computing in High Energy and Nuclear Physics (CHEP09), Prague, Czech Republic, 2009.

[5] The CMS Collaboration. *The CMS Silicon Strip Tracker Operation and Performance with Cosmic Rays in* $3.8\,\mathrm{T}$ *Magnetic Field*, CMS-CFT-09-002, to be submitted to JINST, 2009.

[6] V. Ciulli et al. *Determination of the Lorentz Angle in Microstrip Silicon Detectors with Cosmic Muons*, CMS Note 2008/006, 2008.

[7] CMS Collaboration. *Alignment of the CMS Inner Tracking System with Cosmic Ray Particles*, CMS-CFT-09-003, to be submitted to JINST, 2009.